Direct and Heterodyne Response of Quasi Optical Nb Hot-Electron Bolometer Mixers Designed for 2.5 Thz Radiation Detection

W.F.M. Ganzevles[†], J.R. Gao[§], W.M. Laauwen[§], G. de Lange[§]
T.M. Klapwijk[†] and P.A.J. de Korte[§]
Department of Applied Physics and Delft Institute for Microelectronics
and Submicron Technology (DIMES),
[†]Delft University of Technology,
Lorentzweg 1, 2628 CJ Delft, The Netherlands
[§]Space Research Organization of the Netherlands,
Postbus 800, 9700 AV Groningen, The Netherlands

Abstract

We measure the direct response of a Nb diffusion-cooled hot electron bolometer mixer in a frequency range between 0.5 THz and 3.5 THz. The mixer consists essentially of a twin slot antenna, a co-planar waveguide transmission line and a Nb superconducting bridge. It is designed for use in receivers with astronomical and atmospherical applications around 2.5 THz. We calculate the impedance of the antenna, the transmission line and the bridge separately using models which are developed for frequencies below 1 THz and predict the direct response of the mixer. We demonstrate that these models can be applied to much higher frequencies. However, the measured central frequency is 10-15% lower than predicted. Using a far infrared (FIR) laser, the device can be fully pumped at 2.5 THz. A preliminary Y-factor measurement shows a corrected noise temperature of 4700 K.

1 INTRODUCTION

Astronomic and atmospheric observations in the THz frequency range require highly sensitive radiation detectors. Until recently, Schottky-diodes were the only heterodyne detectors available. Although well understood and not dependent on cryogenic equipment, they show fairly high noise levels. Superconductor-Insulator-Superconductor (SIS) mixers have shown very high sensitivity up to the superconducting gap frequency of Nb, about 700 GHz. At higher frequencies, the losses in both the junction itself and the coupling structures between the antenna and junction increases considerably. Although a lot of effort is dedicated to improvement of the coupling structures by using superconductors with a higher gap, like NbTiN, the upper limit of SIS mixers is considered to be about 1.3 THz. Above that, superconducting hot-electron bolometer mixers (HEBMs) are the heterodyne

detector of choice. The mixing element in these devices is a short superconducting strip, contacted by normal metal cooling pads.

Since there is an interesting spectral line of the hydroxyl-group around 2.5 THz, much attention has been paid to heterodyne detection at this frequency. Several groups have reported heterodyne response at that frequency, some with very good sensitivity (Refs. 1, 2, 3).

The sensitivity of a receiver is determined by its coupling efficiency from free space to the microbridge, its intrinsic noise and its conversion gain. In this work, we focus on the coupling efficiency: is it possible to describe the frequency response of an HEB in terms of a relatively straightforward model and if so, how can we use this model to improve the coupling and ultimately reduce the receiver noise? In this work, we also describe the first heterodyne measurement at 2.5 THz performed using the far infra-red (FIR) laser at SRON.

This paper describes the direct and heterodyne response of quasi optical (QO) HEBMs around 2.5 THz. Part of this work has been described in a separate paper (Ref. 4). It is organized as follows: we will first describe the device layout and secondly, we outline the model we use to predict the direct response of the HEB as a function of frequency. Thirdly, we address the device fabrication and DC characteristics. After a description of the radiofrequency (RF) setup, we compare the direct response as measured in a Fourier Transform Spectrometer (FTS) with the predictions of our model. Then we describe the results of a heterodyne experiment. Lastly, we discuss the results obtained, after which conclusions are drawn.

2 DEVICE LAYOUT

Fig. 1 shows a scanning electron microscopy (SEM) micrograph of a mixer designed for 2.5 THz. It consists of a twin slot antenna, a co-planar waveguide (CPW) transmission line and a Nb microbridge. The twin slot antenna is formed by two gaps in the Au ground plane. The CPW transmission line is used to match the impedance of the antenna to that of the bridge, thus feeding the signal from the antenna to the microbridge.

On one end, the CPW is terminated by the low (practically zero) impedance of the antenna ground plane. On the other end, the CPW transmission line is connected to the intermediate frequency (IF)- and direct current (DC) bias contact via a quarter wavelength ($\frac{1}{4}\lambda$) RF reflection filter, preventing RF radiation from leaking into the IF chain. The $\frac{1}{4}\lambda$ sections are also made of CPW lines. A similar structure was used at 2.5 THz by Karasik et al. (Ref. 1). The fixed polarization, narrow bandwidth, reasonably high gaussicity and efficiency make the twin slot a suitable antenna for application in receivers for use on a telescope.

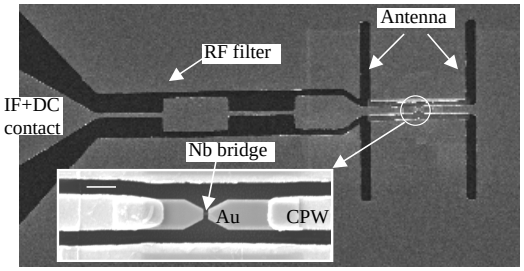

Figure 1: *SEM micrograph of a twin slot antenna coupled Nb HEBM. The nominal slot length L, width w and separation s are 36.0 μm, 1.8 μm, 19.2 μm, respectively. The Nb microbridge and part of the CPW transmission line are shown in the inset, where the bar represents 2 μm.*

3 DEVICE MODELING

A coupling structure similar to the one we use has been applied in a Schottky-mixer at 250 GHz (Ref. 5). A twin slot antenna combined with a microstripline has been used for a SIS mixer around 1 THz (Refs. 6, 7). These studies show that twin slot antennas can be used and modeled up to 1 THz. However, the results of Karasik et al. and Ganzevles et al. (Refs. 1, 8) suggest that the high-frequency behavior is not well understood. Both authors see a considerable downshift of f_{center}. Therefore, in this paper we compare the direct response of the detector as measured in an FTS with the response predicted by a model based on the coupling of successive impedances.

The direct response in current $\Delta I(f)$ of an HEBM measured in an FTS can be described by

$$\Delta I(f) = S\eta_{\mathrm{int}}\eta_{\mathrm{opt}}\eta_{\mathrm{FTS}}P_l, \tag{1}$$

where S is the current responsivity of the microbridge,

η_{int} the intrinsic coupling efficiency of the mixer, η_{opt} the combined transmission of the window and heat filter, η_{FTS} the power transfer function of the FTS. P_{l} is the power spectrum of the lamp. The current responsivity S is considered to be frequency independent as long as the frequency is higher than the superconducting gap frequency, which is justified for our devices. However, the value of S is expected to depend on the mode of operation. If the operating temperature is close to T_c, the detector is operated in the 'transition edge'-regime (Ref. 9). Otherwise, the detector is in the electronic hot-spot regime (Ref. 10). P_{l} is assumed to be a slowly varying function of frequency and can be considered constant throughout the frequency range of interest. The transmission of the lens is not included in equation 1 since it is assumed frequency independent (Ref. 11). Thus, the measured relative response reflects the product of η_{int}, η_{opt} and η_{FTS}.

The direct response is measured at a constant bias voltage. The signal from the lamp is chopped with a frequency of 16 Hz and $\Delta I(f)$ is measured using a lock-in

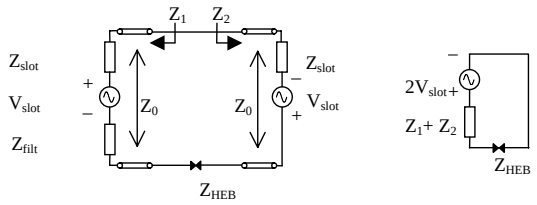

Figure 2: *Equivalent circuit of the antenna-filter-CPW-HEB combination. The antenna is modeled as a voltage source in series with its impedance.*

amplifier. The FTS is operated in a step-and-integrate mode with an integration time of 2 sec. The spectrum is obtained by Fourier transforming the interferogram, which is apodized using a sinusoidal apodization function. The measurements are performed at a temperature close to the superconducting critical temperature T_c.

We start by describing the model to calculate the intrinsic coupling efficiency $\eta_{\rm int}$ of the mixer, namely the power transmitted from the antenna to the bridge. To calculate $\eta_{\rm int}$, we consider each single slot antenna as a voltage generator in series with the antenna impedance. The RF choke filter is assumed in series with one voltage generator/antenna impedance.

As can be seen in Fig. 2, on one side, the microbridge sees an impedance Z_1 equal to the added filter- and antenna slot impedance transformed by the CPW transmission line. On the other side, only the transformed antenna slot impedance Z_2 is present. A similar approach is used for a Schottky-mixer by Gearhart and Rebeiz (Ref. 5). The intrinsic frequency-dependent coupling between the embedding impedance, $Z_{\rm embed} = Z_1 + Z_2$, seen at the bridge terminals and the bolometer impedance $Z_{\rm HEB}$ can now be calculated using

$$\eta_{\rm int} = 1 - \left| \frac{Z_{\rm HEB} - Z_{\rm embed}}{Z_{\rm HEB} + Z_{\rm embed}} \right|^2 . \qquad (2)$$

The impedance of the antenna as a function of frequency is calculated using a moment method in the Fourier transform domain, developed by Kominami et al. (Ref. 12). In the simulation of $\eta_{\rm int}$ we take into account the decrease of the antenna beam efficiency when the frequency is much higher than the design frequency. This effect suppresses the appearance of the second antenna resonance (Ref. 13). The characteristic impedance Z_0 of the CPW transmission line is calculated for several widths of the center conductor and the gap using a software package (MOMENTUM, Ref. 14). It is important to note that the impedances of both the antenna and the CPW are calculated for *printed slots* at the interface between two semi-infinite regions, air and substrate. Basically, the thickness of the metal layer is fully neglected. Because of this, the effective relative dielectric constant $\varepsilon_{\rm eff}$ is $(\varepsilon_{\rm r,\,Si} + \varepsilon_{\rm air})/2$, where $\varepsilon_{\rm r,\,Si}$ and $\varepsilon_{\rm air}$ are the relative dielectric constant of the Si substrate and air, respectively.

The bolometer impedance Z_{HEB} can be expressed as (Ref. 15)

$$Z_{\mathrm{HEB}} = Z_S \frac{l}{d} + Z_l, \tag{3}$$

where Z_S is the surface impedance of the superconducting bridge, l and d are its length and width and Z_l the impedance due to the geometrical inductance of the bridge. Z_S reduces to the square resistance $R_\square$ when the frequency is higher than the superconducting gap frequency of the bridge and the film thickness is much smaller than the skin depth (Ref. 16). Furthermore, Z_l is small, on the order of $1\imath\ \Omega$ for our device. Therefore, Z_{HEB} in practice equals the normal state resistance R_{N}. The effective impedance of the 4-section RF filter is calculated by loading each $\frac{1}{4}\lambda$-CPW section with the effective impedance of its predecessor.

Based on this model we find the maximum coupling efficiency at 2.5 THz for the following mixer geometry: for the antenna we choose length L, separation s and slot width w equal to $0.30 \cdot \lambda_0$, $0.16 \cdot \lambda_0$ and $0.05 \cdot$L, respectively. Here λ_0 is the free-space wavelength (120 μm at 2.5 THz). For the CPW transmission line we choose the center conductor width to be 2 μm and the width of both gaps 0.5 μm, giving Z_0 equal to 39 Ω. For optimal coupling, R_{N} of the bridge is assumed to be 75 Ω. Using these parameters, we predict a maximum value for $\eta_{\mathrm{model,int}}$ of 90%.

4 DEVICE FABRICATION

A fabrication process for Nb HEBMs has been developed using two-step electron beam lithography (EBL) to define both bridge length and width. Deep UV lithography is used to define the layer containing the antenna, CPW, filter etc. In this section, we shortly sketch the fabrication process of the device and present DC measurements.

We use a double-sided polished Si substrate (300 μm thick) with a high resistivity ($\rho = 3 - 5k\Omega$cm). In the first step, 75 nm thick Au squares are DC sputtered. These are used as alignment markers in subsequent optical and e-beam lithography steps. Then we deposit 12 nm Nb using magnetron sputtering. Using a lift-off mask, only patches with a size of 12 μm $\times$ 12 μm are covered. In this way, only a small fraction of RF current has to run in lossy Nb. Furthermore, it decreases the amount of Nb to be opened up for etching, thus reducing the writing time of the EBL machine.

Au cooling pads are patterned using EBL in a double layer of PMMA as a lift-off mask. To achieve a high interface transparency, RF sputter cleaning of the Nb in an Ar-plasma is used to remove its native oxide. In situ, ~ 10 nm Au is sputtered. Then, 90 nm Au is deposited in an e-beam evaporator at a pressure of 2×10^{-6}mbar. The antenna, CPW and filter are defined using a lift-off mask in Shipley DUV III-resist. This step requires the use of DUV lithography because of the 0.5 μm slots in the CPW structure. 5 nm Al plus 10 nm Au is sputtered, after

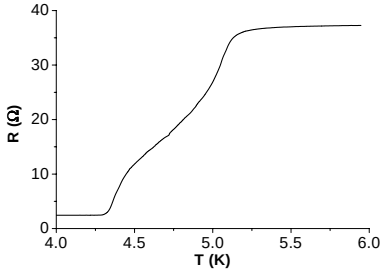

Figure 3: *RT-curve of a typical HEBM.*

which 160 nm Au is evaporated under similar conditions as the cooling pads. As a last optical step, we sputter deposit 100 nm Nb on the IF CPW-transmission line.

For the definition of the bridge width we follow the approach of Wilms Floet et al. (Ref. 17): a PMMA bridge is defined using EBL. Only the Nb parts that have to be etched are opened up, see Fig. 1. In a mixture of CF_4+3%O_2, the Nb is reactive ion etched. We monitor the process by measuring the optical reflectivity of the Nb on the Si substrate by using a laser endpoint detection system. Using this process we are able to produce Nb bridges as narrow as 60 nm.

During processing, all devices are electrically shorted. While dicing in tap water (to avoid electric discharge), these shorts are opened. Therefore, all further handling must be done with extreme care to prevent damage due to electrostatic discharge. After wire bonding, DC measurements are performed in a metal vacuum can immersed in liquid He. Devices suitable for RF measurements are selected based on IV- and RT curves.

The Nb layer in which the bridge is defined has a residual resistance ratio (RRR) equal to 1.5 and $R_{\square,\mathrm{Nb,10K}} = 33\ \Omega$, measured on a large structure. The ground plane (Au, 175 nm) is found to have an RRR of 3.5 and a square resistance $R_{\square,\ \mathrm{Au}}$ of 0.1 Ω at 4 K.

As can be seen in Fig. 3, the critical temperature of the Nb bridge $\mathrm{T_{c,bridge}}$ is 4.8 K. For Nb under the cooling pads $\mathrm{T_{c,pads}}$ is found to be 4.4 K. Both values are considerably lower than those found in literature (Refs. 1,18,19). We suspect that this is caused by the interference of processing different materials in the same sputtering chamber.

We observe a critical current density j_c of 2×10^{10} $\mathrm{Am^{-2}}$ at a temperature of about 3.5 K. An unpumped IV-curve of an HEBM (nominally 250 nm long, 250 nm wide, 12 nm thick) is shown together with pumped curves in Fig. 6 (dashed line).

A QO mixer block has been designed and built as described in Ref. 20 to feed signal from free space to the mixer chip. The chip containing the mixer is glued in the second focus of a hyperhemispherical, high-resistivity Si lens. Before applying glue, we align the antenna to the optical axis (accuracy better than 5 μm) by moving the chip to the center of the lens using micrometers .

The lens itself is held in a copper block. To obtain good thermal contact, 4 springs press the lens softly into the In foil or vacuum grease between the flange of the lens and the Cu block. We find the temperature of the lens to be 4.8 K, without pumping the He-bath.

The block is bolted to the cold plate of a standard 8" dewar, applying a small amount of vacuum grease for thermal contact. Connection to a standard IF-chain (Ref. 21), centered at 1.4 GHz, is made by wire bonding to a microstrip line on an epoxy printed circuit board, 0.5 mm thick, $\varepsilon_{\mathrm{r,\,PCB}} = 4.7$), having < -15 dB reflection over a bandwidth of over 4 GHz. A standard SMA-connector is soldered to its end to connect to the IF chain.

The window of the dewar is made of 40 μm Mylar. We use Zitex (Ref. 22) as an IR filter at 77 K. The transmissivity of these materials as a function of frequency is measured in an FTS. Using a description in terms of a Fabry-Perot etalon, a fit to these measured data is generated. From the period of the transmission oscillations (see Fig. 4), we determine ε_r of the sheet once the thickness is accurately known. The loss factor is determined from the damping in the oscillation maxima. Curves showing the calculated transmissivity as a function of frequency obtained from these measurements are shown in Fig. 4. Although strictly speaking the Zitex does not act as an FP, the data are accurately described by the fit. Table 1 shows the data we obtain for several optical materials of interest in this frequency range.

In order to verify the predictions of the model described above, we measure the frequency dependent response of the mixer using the HEB as a direct detector in

Table 1: *Optical properties of window- and filter materials. The table gives empirical values for β and γ in the description for the absorption coefficient $\alpha(f) = \beta \cdot (\mathrm{f(THz)})^{\gamma}\,[\mathrm{m}^{-1}]$. The absorption factor is then given by $a = e^{\alpha \cdot \delta/2}$, with δ the effective material thickness (i.e. taking into account the angle of incidence).*

	n	β	γ
Mylar	1.72	600	1.2
Zitex G104	1.20	40	2.4
Kapton	1.76	480	1.2
Black Polyethylene	1.50	450	1.7

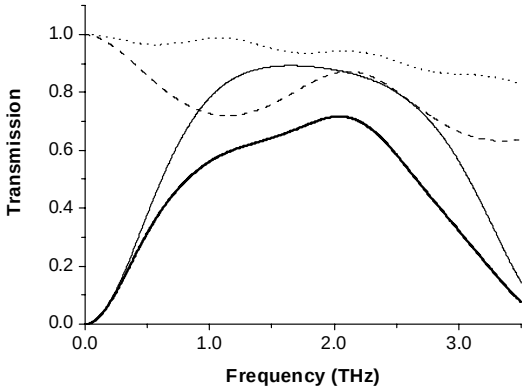

Figure 4: *Calculated transmission of the beam splitter* in an interferometer *(thick solid curve), transmission of the 40 μm Mylar vacuum window (thin dotted curve) and Zitex G104 (thin dashed curve) as a function of frequency. The thick solid line represents the product of the three. The frequency-dependence of the lamp and thin lens in the FTS are not taken into account. The calculations are based on the measured values quoted in Table 1.*

an FTS. The FTS measurement setup consists of a Michelson interferometer with a chopped Hg arc lamp providing broadband THz radiation. One of the mirrors is fixed, while the other can be moved over a range of 32 mm with an accuracy of 5 μm. These parameters give a maximum spectral resolution and frequency range of 5 GHz and 16 THz, respectively. To remove effects of absorption due to water, the whole optical path is in vacuum. For the beam splitter in the FTS (a Mylar sheet, 25 μm thick) the transmissivity vs. frequency is calculated. To do this, we consider it as a beam splitter *in an interferometer* with finite thickness and loss, i.e. taking into account the interference from the waves in both arms (see, e.g. Refs. 23 and 24). For this, we again use the data obtained from the transmission measurements. The thin solid line in Fig. 4 shows the transmission of the beam splitter (Mylar, 25 μm thick) in the FTS.

Heterodyne measurements are done using a FIR laser as a local oscillator (LO) source. The first trap of this system is a CO_2 laser. This laser pumps a FIR ring laser, containing methanol.

A standard hot/cold setup is used as a calibrated source for Y-factor measurements. Systematic measurements require a fairly stable LO signal for longer periods of time (typically a few minutes). Since the LO power was only stable for several tens of seconds, manual Y-factors have been obtained only.

6 DIRECT RESPONSE MEASUREMENTS

Two similar mixers designed for 2.5 THz are measured. Fig. 5 shows a typical measured relative direct response. To obtain the measured $\eta_{\rm int}$, we divide the

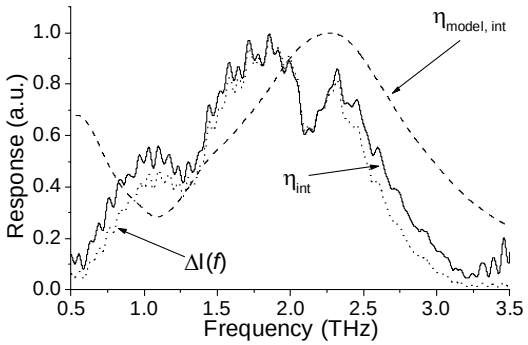

Figure 5: *Direct response of the HEBM designed for 2.5 THz as a function of frequency. The dotted line gives the measured direct response $\Delta I(f)$, reflecting the product of intrinsic coupling efficiency $\eta_{\rm int}$, the combined transmission of the window and heat filter $\eta_{\rm opt}$ and the power transfer function of the FTS $\eta_{\rm FTS}$. The solid line represents the experimental $\eta_{\rm int}$, while the dashed line represents the theoretical prediction $\eta_{\rm model,int}$. All curves are normalized to their maximum value.*

direct response by the product of $\eta_{\rm opt}$ and $\eta_{\rm FTS}$, as shown in Fig. 4. The frequency dependence of the thin lens in the FTS is not considered. The intrinsic response $\eta_{\rm int}$ is also shown in Fig. 5. We find a peak response frequency (the average of the 3 dB values) of 1.9±0.1 THz from the intrinsic mixer response. The 3 dB bandwidth is about 1.3 THz. The unexpected dip around 2.1 THz is not understood but may be due to the FTS lamp (Ref. 25).

To understand this result we calculate the theoretical response $\eta_{\rm int,model}$ using the model described above. Since the actual device parameters differ from those in the initial design, the calculation of the $\eta_{\rm int,model}$ shown in Fig. 5 is done using the actual values, namely $R_{\rm N} = 41\ \Omega$ and $Z_0 = 46\ \Omega$ for the CPW transmission line (Ref. 14) because of a larger gap (0.8 μm).

The model predicts a peak response frequency of 2.3 THz and a 3 dB bandwidth of 1.3 THz. The overall response predicted coincides well with the measured curve if a frequency down shift of about 300 GHz is introduced. By doing this, we infer a peak frequency of 2.0 THz from the measured $\eta_{\rm int}$, consistent with the value determined from the 3 dB points.

We also calculate the relative direct response of the same mixer in an alternative way using Momentum. The result is in general consistent with the simulation shown in Fig. 5. The peak response however is 2.1 THz, also higher than what we measured.

7 HETERODYNE MEASUREMENTS

Heterodyne measurements are performed at a bath temperature of about 3 K. As an LO, the FIR laser is set at a spectral line of methanol at 2.5 THz. The signal

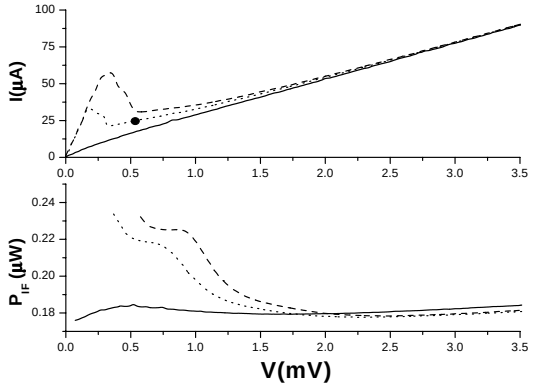

Figure 6: [a)] *Current vs voltage curve for a typical HEBM. The dashed line represents the unpumped curve, the dotted line is optimally pumped and the solid line is overpumped. The dot gives the point where the best Y-factor (0.12 dB) has been measured. Note the series resistance of* 5 Ω *indicated by the slope in the IV curve near zero bias. This is due to the filter and IF contact. For this device,* R_N *equals* 41 Ω. [b)] *The IF output power* P_{IF} *vs voltage for the same device. The curves correspond to the ones in Fig. 6*[a]

is coupled into the dewar via a 15 μm Mylar beam splitter. The transmission of a Mylar splitter at 45° is about 56%. For this particular measurement, the output power of the laser did not allow us to use a thinner splitter. Therefore, we correct the measured noise temperature T_N for the splitter.

At an IF of 1.4 GHz, the best Y-factor obtained is 0.12 ± 0.04 dB. This corresponds to a corrected T_N of 4700 K, about 3 times state of the art for heterodyne receivers at this frequency (Refs. 2, 3). Careful examination of the IV-bias point on an oscilloscope confirms that the bias point is not influenced by the hot/cold load directly, i.e. there is no direct detection. Since the LO is only stable over several tens of seconds, no systematic measurements have been performed to find the optimal bias point, operating temperature or LO power.

8 DISCUSSIONS

Systematic research to the direct response of QO HEBMs has been performed. The measured direct response is compared to the predictions by a simple model based on the coupling of impedances. The influence of the optics in the setup is described based on experimental data of the materials used. The quantitative difference between the measured peak frequencies and those predicted in our calculations occurs only around 2.5 THz but not at low frequencies. We have measured and analyzed similar mixers designed for 1 THz, showing good agreement between measured and predicted response. Although our experimental study does not reveal the origin of this discrepancy, we suggest that the difference is caused by neglecting the finite thickness of the metal layer. For our devices, the thickness

of the metal layer has become comparable to the gap width of the CPW. For the antenna slots at 2.5 THZ, this is also the case. Reasoning qualitatively, this causes a considerable fraction of the field to run in the gap between the slot walls, giving rise to an ε_{eff} lower than assumed for a CPW slot in a metal film with zero thickness. This, in its turn, causes a rise of the characteristic impedance of the CPW lines. Calculations show that a change in characteristic impedance has more influence at 2.5 THz than at 1 THz. Furthermore, the ratio of metal layer thickness over slot width in the antenna slots is larger in the 2.5 THz device. We suppose this changes the antenna impedance more than in the 1 THz device. Both these effects give rise to a more pronounced shift in peak frequency at 2.5 THz than at 1 THz. In order to improve the accuracy of the present model, it would be worthwhile investigating the influence of the thickness of the metal layer.

It becomes clear now that the mixer designed using the present model will not lead to a peak response at 2.5 THz. To achieve ultimate sensitivity at 2.5 THz one can design a mixer in an engineering way by reducing the antenna size by 15% and the CPW gap size to 0.3 μm. The impedance of the HEB device is kept at a practical value of $\sim$40 Ω. Our calculations show that this does not change the peak coupling efficiency, but the size reduction may affect other properties of the antenna. A similar experimental approach has been made by Wyss et al. (Ref. 2).

The Y-factor obtained in heterodyne mode is expected to increase if the coupling scheme can be optimized as described above. Another improvement in Y-factor may come from improving the stability of the LO. Long chopped or even manual scans of the IF output power or Y-factor are expected to be possible, allowing systematic research on the optimal operating conditions of these HEBMs.

9 CONCLUSIONS

In conclusion, we have measured the direct response of Nb HEBMs with a twin slot antenna/CPW transmission line combination around 2.5 THz and compared the results to the present model. The influence of the receiver optics is calculated based on empirical data from FTS measurements. This allows us to take into account the frequency dependence of the transmission due to the optics. We convincingly show that the measured direct response is 10-15% lower in frequency than predicted by the model, although the overall shape of the spectrum agrees with the prediction. Preliminary Y-factor measurements show a noise temperature of 4700 K.

10 ACKNOWLEDGEMENTS

We thank J. Zmuidzinas for useful discussions and making the computer code to calculate the antenna impedance available. M.J.M.E. de Nivelle is acknowledged

for his efforts to make the laser LO ready for heterodyne measurements. Helpful discussions with W. Jellema, N.D. Whyborn, D. Wilms Floet and A. Baryshev are acknowledged. This work is financially supported by the Stichting voor Technische Wetenschappen, which is part of the Nederlandse Organisatie voor Wetenschappelijk Onderzoek, and by ESA under contract no. 11738/95/NL/PB.

REFERENCES

[1] B.S. Karasik, M.C. Gaidis, W.R. McGrath, B. Bumble, and H.G. LeDuc. IEEE Trans. on Appl. Supercond., **7**:3580, 1997.

[2] R.A. Wyss, B.S. Karasik, W.R. McGrath, B. Bumble, and H. LeDuc. Proceedings of the 10^{th} International Symposium on Space Terahertz Technology, Charlottesville, VA, March 16-18, 1999, pages 215–228, 1999.

[3] P. Yagoubov, M. Kroug, H. Merkel, and E. Kollberg. Proceedings of the 10^{th} International Symposium on Space Terahertz Technology, Charlottesville, VA, March 16-18, 1999, pages 238–246, 1999.

[4] W.F.M. Ganzevles, L.R. Swart, J.R. Gao, T.M. Klapwijk, and P.A.J. de Korte. To appear in Appl. Phys. Lett., May 2000.

[5] S.S. Gearhart and G.M. Rebeiz. IEEE Trans. on Microwave Theory Tech., **42**:2504, 1994.

[6] J. Zmuidzinas and H.G. LeDuc. IEEE Trans. on Microwave Theory Tech., **40**:1797, 1992.

[7] M. Bin, M.C. Gaidis, J. Zmuidzinas, T.G. Phillips, and H.G. LeDuc. Appl. Phys. Lett., **68**:1714, 1996.

[8] W.F.M. Ganzevles, J.R. Gao, D. Wilms Floet, G. de Lange, A.K. van Langen, L.R. Swart, T.M. Klapwijk, and P.A.J. de Korte. Proceedings of the 10^{th} International Symposium on Space Terahertz Technology, Charlottesville, VA, March 16-18, 1999, pages 247–260, 1999.

[9] D. Wilms Floet, J.J.A. Baselmans, T.M. Klapwijk, and J.R. Gao. Appl. Phys. Lett., **73**:2826, 1998.

[10] D. Wilms Floet, E. Miedema, T.M. Klapwijk, and J.R. Gao. Appl. Phys. Lett., **74**:433, 1999.

[11] D.F. Filipovic, S.S. Gearhart, and G.M. Rebeiz. IEEE Trans. on Microwave Theory Tech., **41**:1738, 1993.

[12] M. Kominami, D.M. Pozar, and D.H. Schaubert. IEEE Transactions on Antennas and Propagat., **33**:600, 1985. We used a computer code of this method supplied by Zmuidzinas and Chattopadhyay.

[13] J. Zmuidzinas. Private communication.

[14] Hewlett Packard Advanced Design Software, Momentum Planar Solver.

[15] J. Mees, M. Nahum, and P.L. Richards. Appl. Phys. Lett., **5**:2329, 1991.

[16] S. Sridhar. J. Appl. Phys., **63**:159, 1988.

[17] D. Wilms Floet, J.R. Gao, W. Hulshoff, H. van de Stadt, T.M. Klapwijk, and A.K. Suurling. *IOP Conf. Series 158, edited by H. Rogalla and D.H.A. Blank*, page 401, 1997.

[18] D. Wilms Floet, J.J.A. Baselmans, J.R. Gao, and T.M. Klapwijk. Proceedings of the 9^{th} International Symposium on Space Terahertz Technology, Pasadena, CA, March 17-19, 1998, 1998.

[19] P.J. Burke, R.J. Schoelkopf, D.E. Prober, A. Skalare, B.S. Karasik, M.C. Gaidis, W.R. McGrath, B. Bumble, and H.G. LeDuc. J. Appl. Phys., **85**:1644, 1999.

[20] Technical Note I: Hot Electron Bolometer Mixer for 2.5THz, Contract no. 11738/95/NL/PB. Technical report, ESA, 1998.

[21] The IF chain consists of a Berkshire cryo-amplifier (44dB), an isolator, room temperature amplifier (44dB), band pass filter (80 MHz at 1.4 GHz) and a Hewlett Packard power meter. The total gain is 79dB.

[22] Zitex G104: Norton Performance Plastics, Wayne, New Jersey, (201)696-4700.

[23] R.J. Bell. Introductory Fourier Transform Spectroscopy. Academic Press, 1972.

[24] L.R. Swart. Analysis of the direct response of twin slot antenna coupled Nb HEB mixers designed for 2.5 THz detection. MSc. thesis, University of Groningen, 1999.

[25] We do not attribute the dip to the device since devices having different types of antenna and transmission lines show the dip at the same frequency.